

Published in final edited form as:

Neuron. 2010 December 9; 68(5): 964–977. doi:10.1016/j.neuron.2010.11.017.

***Drosophila* pacemaker neurons require G-protein signaling and GABAergic inputs to generate 24hr behavioral rhythms**

David Dahdal¹, David C. Reeves^{2,3}, Marc Ruben¹, Myles H. Akabas², and Justin Blau¹

¹ Department of Biology, New York University, 100 Washington Square East, New York, NY 10003

² Departments of Physiology & Biophysics and Neuroscience, Albert Einstein College of Medicine of Yeshiva University, Bronx, NY 10461

³ ARMGO Pharma Inc. 777 Old Saw Mill River Road, Tarrytown, NY 10591

Summary

Intercellular signaling is important for accurate circadian rhythms. In *Drosophila*, the small ventral lateral neurons (s-LN_vs) are the dominant pacemaker neurons and set the pace of most other clock neurons in constant darkness. Here we show that two distinct G-protein signaling pathways are required in LN_vs for 24hr rhythms. Reducing signaling in LN_vs via the G-alpha subunit Gs, which signals via cAMP, or via the G-alpha subunit Go, which we show signals via Phospholipase 21c, lengthens the period of behavioral rhythms. In contrast, constitutive Gs or Go signaling makes most flies arrhythmic. Using dissociated LN_vs in culture, we found that Go and the metabotropic GABA_B-R3 receptor are required for the inhibitory effects of GABA on LN_vs and that reduced GABA_B-R3 expression *in vivo* lengthens period. Although no clock neurons produce GABA, hyper-exciting GABAergic neurons disrupts behavioral rhythms and s-LN_v molecular clocks. Therefore, s-LN_vs require GABAergic inputs for 24hr rhythms.

Introduction

Circadian rhythms are found in organisms as diverse as plants and humans. In all organisms so far studied, these ~24hr rhythms are driven by intracellular molecular clocks that consist of transcriptional/translational feedback loops with additional post-translational regulation. The importance of molecular clocks in determining period length is exemplified by the numerous clock gene mutations that alter molecular clock speed and behavioral rhythms (reviewed by Allada et al., 2001). Since many mammalian cells show rhythmic clock gene expression in culture, intracellular clocks are often considered cell-autonomous (Balsalobre et al., 1998; Welsh et al., 1995).

However, intercellular communication is also important for circadian rhythms. For example, signals from master pacemaker neurons in the mammalian suprachiasmatic nucleus (SCN) regulate the phase of clocks in peripheral organs (Reppert and Weaver, 2002). Coupling of pacemaker neurons within the SCN is also important because individual pacemaker neurons

© 2010 Elsevier Inc. All rights reserved.

Corresponding author: justin.blau@nyu.edu.

Publisher's Disclaimer: This is a PDF file of an unedited manuscript that has been accepted for publication. As a service to our customers we are providing this early version of the manuscript. The manuscript will undergo copyediting, typesetting, and review of the resulting proof before it is published in its final citable form. Please note that during the production process errors may be discovered which could affect the content, and all legal disclaimers that apply to the journal pertain.

from a single animal display a range of periods of electrical rhythms when dispersed in culture, whereas only one period is measured in SCN explants and animals (Herzog et al., 1998; Liu et al., 1997). Similarly, deletions of either *mPeriod1* (*mPer1*) or *mCryptochrome1* (*mCry1*) clock genes dramatically weakened molecular rhythms in individual dissociated SCN cells but had minimal effects on molecular rhythms in SCN explants or animal behavioral rhythms (Liu et al., 2007). Presumably, coupling between cells rescues the genetically weakened individual SCN oscillators and suggests that signaling between clock neurons is essential for robust SCN rhythms.

Further support for SCN intercellular communication comes from *VPAC₂R*^{-/-} mice. *VPAC₂R* encodes a G-protein coupled receptor (GPCR) expressed by many SCN neurons and is activated by the neuropeptides VIP and PACAP (Harmar et al., 1998). *VPAC₂R*^{-/-} mutant mice are behaviorally arrhythmic (Harmar et al., 2002) and most neurons in SCN slices from *VPAC₂R*^{-/-} mutants lose *mPer1::luciferase* rhythms (Maywood et al., 2006). Thus disrupting a membrane-bound receptor that presumably acts as an input to SCN neurons prevented molecular rhythms even though core clock genes were genetically unaffected.

Drosophila have ~150 clock neurons in discrete clusters in the brain, named after their location: In each hemisphere, there are 4 small and 4 large ventral Lateral Neurons (s- and l-LN_vs) that synthesize the key circadian neuropeptide Pigment Dispersing Factor (PDF). There are also: a 5th PDF-negative s-LN_v; 6 dorsal Lateral neurons (LN_ds); 3 Lateral posterior clock neurons (LPNs) and ~50 clock neurons located in three different dorsal clusters (DN₁₋₃). Over-expression of the Shaggy/GSK3 (*Sgg*) kinase only in s-LN_vs speeds up their own molecular clocks and the clocks in most other central brain clock neurons. In contrast, *sgg* over-expression in all clock neurons except LN_vs does not alter the speed of s-LN_v or most other molecular clocks (Stoleru et al., 2005). Therefore s-LN_vs seem to be the master pacemakers in constant darkness (DD) and set the pace for much of the *Drosophila* clock network. Although the ability of individual *Drosophila* clock neurons to generate 24hr rhythms has not been tested in culture, intercellular communication between *Drosophila* pacemaker neurons could explain how molecular and behavioral rhythms persist in DD *in vivo* (Lin et al., 2004; Peng et al., 2003; Yoshii et al., 2009). In contrast, oscillations in peripheral clocks, which are not coupled to each other, dampen in DD (Stanewsky et al., 1997).

Although s-LN_vs are pacemakers in DD, they require signals from their cell membrane for 24hr rhythms. For example, s-LN_v molecular clocks desynchronize and/or run down in DD in *Pdf⁰¹* null mutant flies (Lin et al., 2004; Peng et al., 2003; Yoshii et al., 2009) and run down when hyperpolarized in DD (Nitabach et al., 2002). *Pdf⁰¹* and *PDF receptor (pdfR)* mutant flies are either arrhythmic or have short period behavioral rhythms in DD (Hyun et al., 2005; Lear et al., 2005; Mertens et al., 2005; Renn et al., 1999). Like *VPAC₂R*, the PDFR is a GPCR which signals via cAMP at least *in vitro* (Hyun et al., 2005; Mertens et al., 2005) and LN_vs also seem to respond to PDF (Im and Taghert, 2010; Shafer et al., 2008).

LN_vs also respond to neurotransmitters from other neurons. The Hofbauer-Buchner eyelet photoreceptor cells project to LN_vs and produce acetylcholine (ACh) and histamine (Pollack and Hofbauer, 1991; Yasuyama and Meinertzhagen, 1999). Serotonergic neurons project to adult LN_vs and modulate light entrainment via the metabotropic 5-HT_{1B} receptor in LN_vs (Yuan et al., 2005) and l-LN_vs respond to GABA via the ionotropic GABA_A receptor, RDL, to regulate sleep and arousal (Chung et al., 2009; Parisky et al., 2008). Larval LN_vs, which become the adult s-LN_vs, respond directly to ACh, GABA and glutamate *in vitro* and produce glutamate and GABA metabotropic receptors (Hamasaka et al., 2007; Hamasaka et al., 2005; Wegener et al., 2004). Although glutamatergic and GABAergic neurons project to

larval and adult LN_vs (Hamasaka et al., 2007; Hamasaka et al., 2005), their role in circadian rhythms is largely unknown.

We first addressed the role of GPCRs in s-LN_vs by manipulating G-protein signaling. We focused on two G-protein alpha subunits: G- α 60A (Gs), which activates Adenylate cyclase to produce cAMP; and G- α 47A (Go), whose signaling mechanism was unclear previous to this study, but likely cAMP-independent (Ferris et al., 2006). We found that reduced signaling via either Gs or Go in LN_vs lengthened the period of behavioral rhythms, while constitutively activating Gs or Go made flies largely arrhythmic. In epistasis experiments, expressing the cAMP phosphodiesterase *dunce* (*dnc*) rescued the arrhythmicity of constitutively active Gs and lengthened period when expressed alone, showing that Gs signals via cAMP to regulate period length in LN_vs. Similarly, reducing *Phospholipase C 21C* (*Plc21C*) expression rescued arrhythmicity induced by a constitutively active Go transgene and lengthened behavioral period on its own, indicating that PLC21C lies downstream of Go in LN_vs. Given this previously unsuspected role of Go signaling in maintaining 24hr rhythms in LN_vs, we sought to identify potential receptors and ligands that signal via Go.

We measured Ca²⁺ responses of dissociated LN_vs in culture and found that inhibiting Go made LN_vs unresponsive to GABA but did not affect LN_v responses to ACh or glutamate. We found that GABA likely signals via the metabotropic GABA receptor *GABA_B-R3* in LN_vs since knocking down its expression strongly reduced the response to GABA in culture and lengthened behavioral rhythms in adult flies. Although LN_vs do not produce GABA themselves (Hamasaka et al., 2005), we found that hyper-exciting GABAergic neurons disrupts animal behavioral rhythms and s-LN_v molecular clocks. Therefore s-LN_vs integrate signals from GABAergic neurons as part of a network that generates 24hr rhythms.

Results

Gs-mediated signaling in LN_vs is required for 24hr rhythms

The neuropeptide PDF is the only described signal that s-LN_vs require to maintain synchronous molecular oscillations (Lin et al., 2004; Peng et al., 2003). s-LN_vs likely use PDF to signal to each other since they express PDFR (Im and Taghert, 2010), a GPCR that likely couples to Gs (Hyun et al., 2005; Mertens et al., 2005; Shafer et al., 2008). To test how important Gs signaling in LN_vs is for circadian rhythms, we assayed the behavior of flies with altered Gs expression or activity in LN_vs.

We first measured the locomotor activity in DD of flies in which Gs RNA levels were reduced specifically in LN_vs using two copies of the *Pdf-Gal4* driver to express a previously described *UAS-Gs-RNAi* transgene (Ueno et al., 2006). The average period of these *Pdf > Gs-RNAi* flies was 25.0hr, significantly longer than the 24.0hr or 23.8hr periods of control flies with *Pdf-Gal4* or *UAS-Gs-RNAi* alone (p<.001, Figure 1A and Table1). Next we assayed flies expressing either wild-type Gs or Gs carrying a point mutation that eliminates its intrinsic GTPase activity and makes Gs constitutively active (*UAS-Gs* and *UAS-Gs-GTP* respectively, (Wolfgang et al., 1996). We found that more than 60% of *Pdf > Gs* and *Pdf > Gs-GTP* flies were arrhythmic while the rhythmic flies had normal periods but were only weakly rhythmic – shown by a lower rhythm power than control flies (Figure 1A, Table1). We checked for the presence of s-LN_vs in *Pdf > Gs-GTP* flies, using antibodies to PDF and found that s-LN_vs project normally to the dorsal brain and also express the clock proteins VRI and PER at ZT20 (ZT: Zeitgeber time, time in a 12:12 LD cycle; Figure S1). Therefore the arrhythmicity of many *Pdf > Gs-GTP* flies is not due to loss of s-LN_vs or to visible developmental defects.

cAMP phosphodiesterases, such as DNC, reduce Gs-mediated signaling by hydrolyzing cAMP to AMP. Therefore, we used a *UAS-dnc* transgene (Cheung et al., 1999) to decrease cAMP levels as an independent way to alter Gs signaling activity in LN_vs. We found that *Pdf > dnc* flies had much longer periods than control *UAS-dnc* flies (26.6hr vs. 24.0hr respectively, $p < .001$, Figure 1B and Table 1). We also found that the arrhythmicity caused by expressing GsGTP in LN_vs could be completely rescued by co-expression of *UAS-dnc* but not by co-expressing a control transgene, *UAS-CD8::GFP* (Figure 1C, Table 1). Thus the effects of Gs on circadian rhythms are mediated via cAMP rather than direct effects of activated Gs on ion channels. We also noticed that *Pdf > Gs-GTP + dnc* flies have ~2hr shorter period lengths than *Pdf > dnc* flies, suggesting that cAMP levels help determine period length as in mammals (O'Neill et al., 2008). Similarly, flies with only one copy of *Pdf-Gal4* expressing *UAS-dnc* have shorter periods (25.5hr) than flies with two copies of *Pdf-Gal4* (26.6hr) - presumably the latter have higher DNC levels and lower cAMP levels.

We also tested whether period length could be altered by mis-expressing PDE8, another cAMP-specific phosphodiesterase (Day et al., 2005). We found that *Pdf > Pde8^{EY10946}* flies have longer period rhythms than control flies (25.0hr, Figure 1D, Table 1). We confirmed that this previously uncharacterized *Pde8* P-element insertion that contains binding sites for Gal4 increases *Pde8* RNA levels when activated by a Gal4 driver (Figure 1E). Overall our data show that Gs signaling and cAMP levels in LN_vs are important determinants of period length. Although previous studies in *Drosophila* implicated cAMP-mediated signaling in circadian rhythms (Levine et al., 1994; Majercak et al., 1997), our data point to the LN_vs as the relevant cellular substrate.

Normal Go activity in LN_vs is required for 24hr rhythms

Next we tested if other G-alpha proteins are also important for circadian behavior. One major class of G-proteins is sensitive to Pertussis toxin (Ptx), which specifically inhibits Go signaling in flies (Ferris et al., 2006; Katanaev et al., 2005). Since a Gal4 enhancer trap in the *Go* locus gave expression in s-LN_vs (data not shown), we tested if Go signaling regulates circadian rhythms by expressing a *UAS-Ptx* transgene (Ferris et al., 2006) in LN_vs. The average behavioral period of *Pdf > Ptx* flies in DD is 25.2hr, significantly longer than control flies ($p < .001$, Figure 2A, Table 1). We also used a *UAS-Go* transgene in which a single amino acid change (G203T) reduces Go affinity for GTP and decreases endogenous Go signaling in a dominant-negative manner (*Go-GDP*, Katanaev et al., 2005). *Pdf > Go-GDP* flies also had ~1hr longer period than control flies ($p < .001$, Figure 2A, Table 1). Therefore, inhibiting endogenous Go activity in LN_vs using two independent transgenes lengthened period.

We also assayed behavioral rhythms of flies expressing a constitutively active Go transgene (*Go-GTP*, Katanaev et al., 2005) and found that nearly 50% of *Pdf > Go-GTP* flies were arrhythmic. The remaining rhythmic flies had short period rhythms (22.3hr), although with a weak power (Figure 2A, Table 1). Thus reduced signaling via Go in LN_vs lengthens period, while increased Go signaling leads to arrhythmicity or short periods.

Plc21C lies downstream of Go in LN_vs

Unlike Gs, the signaling pathway downstream of Go in *Drosophila* is unclear. One well-studied pathway downstream of G-proteins involves PLC enzymes, which cleave the phospholipid PIP₂ into second messengers. *Plc21C* is widely expressed in the brain and co-localizes with Go at low resolution (Shortridge et al., 1991).

We hypothesized that the arrhythmicity of *Pdf > Go-GTP* flies should be rescued by reducing downstream signaling as observed with co-expression of *UAS-dnc* with *UAS-*

GsGTP (Figure 1C). Therefore, we measured locomotor rhythms of flies expressing *UAS-Go-GTP* in LN_{ν} s along with either *UAS-dnc* or with an RNAi transgene that targets *Plc21C*. To control for transgene expression levels, we also assayed flies with *Go-GTP* co-expressed with GFP or RNAi to *Germ line transcription factor 1 (Gnf1)*, which is unlikely to be expressed in LN_{ν} s. The results in Figure 2B and Table 1 show that *Pdf > Go-GTP + GFP* and *Pdf > Go-GTP + Gnf1-RNAi* flies were either arrhythmic or had weak rhythms. *Pdf > Go-GTP + dnc* flies had low power short-period rhythms, indicating that Go is unlikely to signal by increasing cAMP in LN_{ν} s. This is consistent with Go acting independently of the cAMP pathway in mushroom bodies (Ferris et al., 2006). Strikingly, all *Pdf > Go-GTP + Plc21C-RNAi* flies had strong rhythms. Since *Plc21C-RNAi* suppressed the *Go-GTP* phenotype, we conclude that *Plc21C* lies downstream of *Go* in LN_{ν} s.

We noticed that *Pdf > Go-GTP + Plc21C-RNAi* flies had slightly longer period rhythms (24.7hr) than control flies. *Pdf > Plc21C-RNAi* flies without *Go-GTP* also have a longer period (25.1hr) than control *Pdf > Gnf1-RNAi* flies (Figure 2C and Table 1), consistent with the long periods seen when *Go* activity is reduced in LN_{ν} s. We confirmed that the *UAS-Plc21C-RNAi* transgene reduced *Plc21C* RNA levels when expressed pan-neuronally (Figure 2D). Thus *Go / PLC21C* signaling is a novel pathway that helps LN_{ν} s drive 24hr behavioral rhythms

These data indicate that *Go* and *Gs* activate distinct signaling pathways. Since combining two mutations that affect different steps in the molecular clock affects period length additively (Lakin-Thomas and Brody, 1985; Rothenfluh et al., 2000), we tested if *Go* and *Gs* pathways act in parallel by measuring the period lengths of flies with both pathways inhibited simultaneously. We found that flies co-expressing *dnc* and *Ptx* in LN_{ν} s have an average period of 28.4hr, significantly longer than either *Pdf > dnc* or *Pdf > Ptx* flies alone ($p < 0.001$, Figure 2D and Table 1). Therefore we conclude that *Gs* and *Go* signaling act in parallel in LN_{ν} s to promote 24hr rhythms.

Inhibiting *Go* slows the molecular clock

Altered period behavioral rhythms are typically associated with changes in the s- LN_{ν} molecular clock. To test this for *Go* signaling, we assayed molecular clock oscillations in *Pdf > Ptx* flies. We dissected adult flies on the third day of DD so that the 1.3hr difference in period length per day would result in a ~4hr shift. We stained fly brains at 4hr intervals for the rhythmically produced clock protein VRI, which is detected during subjective night in wild type flies (Cyran et al., 2003; Glossop et al., 2003).

VRI staining was first detected in control s- LN_{ν} s at CT16, reached peak levels at CT20 and then became almost undetectable by CT24. In contrast, VRI was not clearly detectable in s- LN_{ν} s of *Pdf > Ptx* flies until CT20 and remained at high levels at CT24, before disappearing by CT4 on the next day (Figure 3). Therefore, the s- LN_{ν} molecular clock in *Pdf > Ptx* flies is rhythmic, but its phase is delayed, consistent with long period behavioral rhythms. Thus *GoPLC21C* signaling interacts with core clock components to regulate molecular clock speed.

Go is required for GABA to inhibit LN_{ν} neuronal activity *in vitro*

Although LN_{ν} s are usually considered cell-autonomous oscillators, the involvement of *Gs* and *Go* signaling suggested that they normally receive inputs to generate 24hr rhythms. Given that *Go* signaling was previously unstudied in fly circadian rhythms, we sought to identify ligands and GPCRs which signal via *Go* in LN_{ν} s as the first step towards identifying the neurons which help set molecular clock speed.

For this, we modified the assay of Wegener et al. (2004) that measures Ca^{2+} responses in dissociated larval $\text{LN}_{\text{V}}\text{s}$. We used larval $\text{LN}_{\text{V}}\text{s}$ to be able to use the strong *Pdf-Gal4* driver without needing to distinguish s- and l- $\text{LN}_{\text{V}}\text{s}$ by size. Studying larval $\text{LN}_{\text{V}}\text{s}$ is relevant because they become the adult s- $\text{LN}_{\text{V}}\text{s}$ (Kaneko et al., 1997) and gene expression patterns remain similar between larval $\text{LN}_{\text{V}}\text{s}$ and adult s- $\text{LN}_{\text{V}}\text{s}$ (Nagoshi et al., 2010).

Instead of measuring Ca^{2+} changes via Fura-2, we used the genetically encoded Ca^{2+} indicator *G-CaMP1.6* (Reiff et al., 2005). We found that larval $\text{LN}_{\text{V}}\text{s}$ expressing G-CaMP fluoresce more reliably and strongly than after Fura-2 loading. $10\mu\text{M}$ ACh robustly increased fluorescence (25-80% of baseline) in $>90\%$ G-CaMP+ dissociated $\text{LN}_{\text{V}}\text{s}$ as previously described (Wegener et al., 2004). Fluorescence did not run down during an experiment (Figure 4A, S2-3) allowing a single G-CaMP+ neuron to be recorded for >30 min.

We found a similar concentration-response relationship for ACh in G-CaMP+ neurons as Wegener et al (2004) had found for Fura-2 loaded $\text{LN}_{\text{V}}\text{s}$ (Figure 4C). These Ca^{2+} increases require nicotinic ACh receptor (nAChR) activation since $10\mu\text{M}$ nicotine also increased G-CaMP fluorescence (Figure S2A), as reported by Wegener et al. (2004). Furthermore, applying the nAChR antagonist α -Bungarotoxin (α -Btx) prevented intracellular Ca^{2+} increases when co-applied with ACh (Figure S2A and M. Vömel & C. Wegener, personal communication). α -Btx inhibition on $\text{LN}_{\text{V}}\text{s}$ was reversible (Figure S2A) as previously described in insect cells (Albert and Lingle, 1993).

In agreement with Wegener et al. (2004), we also found ACh-induced intracellular Ca^{2+} increases require extracellular Ca^{2+} (Figure S2B) and are blocked by $30\mu\text{M}$ extracellular Cd^{2+} , which inhibits voltage-gated Ca^{2+} channels (VGCC, Figure S2C). Raising extracellular K^{+} to depolarize $\text{LN}_{\text{V}}\text{s}$ also increased G-CaMP fluorescence to similar levels as ACh (EC_{50} for K^{+} , 30.8 ± 1.2 mM, Figure S3A and data not shown). These data indicate that ACh binds to nAChRs that activate VGCC to allow extracellular Ca^{2+} to enter $\text{LN}_{\text{V}}\text{s}$. For this, nAChRs and VGCCs must be in close proximity at least in dissociated larval $\text{LN}_{\text{V}}\text{s}$ and this system offers a powerful way to study the direct effects of ligands on $\text{LN}_{\text{V}}\text{s}$.

We tested a number of other neurotransmitters, but found no change in G-CaMP-fluorescence in $\text{LN}_{\text{V}}\text{s}$ either during or after applications of $100\mu\text{M}$ GABA, glutamate, glycine, histamine, 5-HT, NMDA or octopamine (data not shown). These high neurotransmitter doses would be expected to give responses if $\text{LN}_{\text{V}}\text{s}$ possess the appropriate receptors. However, it was previously reported that glutamate and GABA decrease Ca^{2+} levels via metabotropic glutamate and GABA receptors ($\text{GABA}_{\text{B}}\text{-Rs}$) in Fura-2 loaded $\text{LN}_{\text{V}}\text{s}$ (Hamasaka et al., 2007; Hamasaka et al., 2005). These receptors are candidates for coupling to Go. Since we could not detect spontaneous activity with GABA and glutamate in dissociated $\text{LN}_{\text{V}}\text{s}$, we co-applied them with ACh to attempt to detect inhibition. We found that co-applying $100\mu\text{M}$ GABA or glutamate almost completely inhibited the Ca^{2+} response to $10\mu\text{M}$ ACh (Figure 4A, 4B).

To test if Go is required for inhibition by GABA and/or glutamate, we compared the responses of control *Pdf > G-CaMP* larval $\text{LN}_{\text{V}}\text{s}$ with $\text{LN}_{\text{V}}\text{s}$ also expressing *UAS-Ptx* (*Pdf > G-CaMP + Ptx*). Both sets of cells responded similarly to ACh applied alone (Figure 4A, B). When ACh was co-applied with $100\mu\text{M}$ GABA, the response of control *Pdf > G-CaMP* $\text{LN}_{\text{V}}\text{s}$ was inhibited by 85%. However, the inhibition by GABA was only 5% in *Pdf > G-CaMP + Ptx* cells (Figure 4A, B). We estimated the GABA IC_{50} for control $\text{LN}_{\text{V}}\text{s}$ as $3.8\mu\text{M}$ whereas GABA did not inhibit the ACh response of *Pdf > G-CaMP + Ptx* $\text{LN}_{\text{V}}\text{s}$ even at 10mM (Figure 4C). Co-applying glutamate with ACh inhibited the ACh-induced Ca^{2+} response in both sets of cells (Figure 4A, B), indicating that Ptx specifically blocks GABA-

mediated inhibition. Since Ptx prevents the Go- $\alpha/\beta/\gamma$ heterotrimer from coupling to activated GPCRs, we propose that metabotropic GABA_B-Rs normally signal via Go in LN_vs. Similar conclusions were made in *Drosophila* olfactory receptor neurons using *UAS-Ptx* (Olsen and Wilson, 2008).

Adult l-LN_vs have functional GABA_A/RDL receptors that are sensitive to picrotoxin and implicated in arousal (Chung et al., 2009; Parisky et al., 2008). However, we found that 4 μ M picrotoxin, which blocks the open channel of GABA_A/RDL receptors, did not alter GABA-inhibition of ACh-induced Ca²⁺ responses in larval LN_vs (Figure S3C). Thus the GABA-mediated inhibition observed here is independent of GABA_A/RDL receptors. The general K⁺ channel inhibitors TEA or Cs⁺ (Hille, 2001) did not affect GABA-mediated inhibition (Figure S3C). Although the sequence of 1 of the 3 *Drosophila* G-protein coupled Inward Rectifier K⁺ channel suggests that it may not be blocked by TEA (Kavanaugh et al., 1991; McCormack, 2003), the lack of an effect of Cs⁺ is consistent with GABA inhibiting LN_vs independently of K⁺ channels.

GABA signals via GABA_B-R3 receptors in LN_vs

Next we sought to identify the GABA_B receptor(s) in LN_vs responsible for GABA-inhibition of ACh. The *Drosophila* genome has three annotated GABA_B-R genes (Mezler et al., 2001): GABA_B-R1 and GABA_B-R2 form a functional heterodimer, while GABA_B-R3 does not dimerize with GABA_B-R1 or R2 and likely interacts with an as yet unidentified additional GABA_BR (Kaupmann et al., 1998; Mezler et al., 2001).

To identify which GABA_B receptor(s) is required in LN_vs, we first used 3-APMPA, an agonist for *Drosophila* GABA_B-R1/2 (Hamasaka et al., 2005; Mezler et al., 2001). 3-APMPA did not alter LN_v Ca²⁺ responses when co-applied with ACh, even at 20 μ M (data not shown), which is more than twice the 3-APMPA reported EC₅₀ (Hamasaka et al 2005). GABA also inhibited LN_v Ca²⁺ responses to ACh when LN_vs expressed a *UAS-GABA_B-R2-RNAi* transgene (Figure 5A) even though this *GABA_B-R2-RNAi* transgene potently reduces *GABA_B-R2* expression (Figure 5B). Since GABA_B-R1 and GABA_B-R2 seem to function together, we conclude that GABA_B-R1/2 is not involved in GABA-mediated inhibition of ACh responses in LN_vs.

GABA_B-R3 expression is enriched ~20-fold in adult s-LN_vs at ZT12 compared to other differentiated neurons (Kula-Eversole et al., 2010). To test a role for GABA_B-R3 in mediating GABA responses in LN_vs, we used a *UAS-GABA_B-R3-RNAi* transgene since there are no pharmacological agents that target GABA_B-R3. We compared the responses of LN_vs from control *Pdf > G-CaMP* larvae and from larvae expressing both *G-CaMP* and *GABA_B-R3-RNAi* transgenes. The results in Figure 5A, S3A and S3B show normal activation by ACh and inhibition by glutamate. However, while GABA inhibited the response of control *Pdf > G-CaMP* LN_vs to ACh by 89%, *Pdf > G-CaMP + R3-RNAi* LN_vs showed only 20% inhibition. We could not detect a significant change in *GABA_B-R3* expression in RNA from whole fly heads when *GABA_B-R3-RNAi* was expressed with *elav-Gal4*. Instead, we measured *GABA_B-R3* RNA levels from adult LN_vs purified via flow cytometry using a *Pdf-RFP* transgene (Blanchard et al., 2010) to sort LN_vs. This technique reliably reports rhythmic clock gene expression in LN_vs (MR, M. Drapeau & JB, manuscript in preparation). The RNA analyzed is likely from a mixture of s- and l-LN_vs. The results in Figure 5C show that *GABA_B-R3* RNA levels are significantly higher in LN_vs isolated from *Pdf-RFP* control flies than in LN_vs from *Pdf-RFP; Pdf > GABA_B-R3-RNAi* flies. Therefore, the *GABA_B-R3-RNAi* transgene reduces *GABA_B-R3* expression. Overall, our data indicate that GABA_B-R3 is the relevant GABA_B receptor that mediates the inhibitory effects of GABA on LN_v Ca²⁺ responses.

To test whether reducing expression of *GABA_B-R3* alters adult behavioral rhythms, we assayed the locomotor activity of flies expressing RNAi against *GABA_B-R3* in adult LN_vs and compared them to flies expressing *GABA_B-R2-RNAi*. The results in Figure 5D and Table 1 show that *Pdf > GABA_B-R3-RNAi* flies had longer periods than *Pdf > GABA_B-R2-RNAi* flies (24.9hr vs 24.3hr respectively, $p < .001$). The long period is consistent with reduced signaling via Go in *Pdf > Ptx* and *Pdf > Go-GDP* flies (Table1). Taken together our results indicate that signaling via *GABA_B-R3* in s-LN_vs helps to generate 24hr rhythms and raise the possibility that GABAergic neurons are part of the circadian network.

Hyper-exciting GABAergic neurons disrupts circadian rhythms

Given the presence of functional *GABA_B-R3* receptors in LN_vs, we asked whether manipulating GABAergic neurons themselves also affects circadian rhythms. We used two Gal4 drivers with regulatory regions from *Glutamate decarboxylase 1 (Gad1)*, which encodes the enzyme that converts Glutamate into GABA, and one with the regulatory region of the *vesicular GABA transporter (vGAT, Fei et al., 2010)*. However, these GABAergic neuron drivers were mainly lethal when crossed to transgenes that ablate, hyperpolarize or hyper-excite neurons or block synaptic release. However, healthy offspring were obtained by crossing *Gad-Gal4* (Mehren and Griffith, 2006) to *UAS-NaChBac2*, which encodes a voltage-gated bacterial Na⁺ channel that hyper-excites neurons (Nitabach et al., 2006; Sheeba et al., 2008). The results in Figure 6A and Table 1 show that *Gad > NaChBac2* flies were either arrhythmic or had significantly weaker rhythms than control flies.

To test if these behavioral phenotypes are due to expression in clock neurons, we crossed *Gad-Gal4* with *GFP* reporter flies. We could not detect GFP expression in any clock neurons (Figure 6B), consistent with no GABA immunoreactivity in clock neurons (Hamasaka et al., 2005). Therefore the disrupted locomotor rhythms in *Gad > NaChBac2* flies are due to hyper-exciting *Gad-Gal4* expressing cells that are not canonical clock neurons.

Altering GABAergic neuron activity changes *Drosophila* sleep levels in LD cycles (Agosto et al., 2008; Parisky et al., 2008). Therefore the altered behavioral rhythms of *Gad > NaChBac2* flies could result from altered arousal mediated via GABAergic neurons. In this scenario, the s-LN_v molecular clocks would be expected to run normally in *Gad > NaChBac2* flies. Alternatively, the weak behavioral rhythms of *Gad > NaChBac2* flies could be at least partly due to increased GABAergic signaling that alters s-LN_v molecular clocks.

To assay the s-LN_v molecular clock, we compared levels of the clock proteins VRI and PER in s-LN_vs of *Gad-Gal4* control flies and *Gad > NaChBac2* flies at 4 different time points on day 3 in DD. Figure 7 shows that overall VRI and PER levels are lower in *Gad > NaChBac2* flies than in control flies. Furthermore, VRI and PER levels are variable between s-LN_vs in the same cluster in *Gad > NaChBac2* brains. For example, VRI was detected in only 2 of the 4 s-LN_vs in the *Gad > NaChBac2* fly shown at CT3 (Figure 7A). We also measured VRI and PER levels in LD cycles and found no significant difference between control and experimental flies (data not shown), indicating that s-LN_vs entrain properly and that light over-rides the effect of hyper-exciting GABAergic neurons. Since molecular rhythms in s-LN_vs are disrupted by hyper-exciting GABAergic neurons, we conclude that normal levels of signaling from GABAergic neurons are necessary for 24hr molecular clock rhythms in s-LN_vs in DD.

Discussion

G-protein signaling in LN_vs

Here we demonstrate the importance of G-protein signaling in s-LN_vs for 24hr rhythms in DD. We show that Gs and Go pathways act in parallel to regulate the s-LN_v molecular clock since simultaneously reducing signaling via Gs and Go lengthens rhythms by more than 4hr. Therefore LN_vs normally require an appropriate level of signaling via Gs and Go to generate 24hr rhythms in DD. Since activation of Gs and Go generates intracellular second messengers, our work adds to the evidence implicating small molecules in regulating molecular clocks across species (Dodd et al., 2007; Harrisingh et al., 2007; O'Neill et al., 2008).

Signaling via Gs in LN_vs

The long-periods we observed with reduced Gs signaling are consistent with four other manipulations of cAMP levels or PKA activity that alter fly circadian behavior. First, long-period rhythms with *dnc* over-expression complement the short periods of *dnc* hypomorphs (Levine et al., 1994) and suggest that the latter are due to loss of *dnc* from LN_vs. *dnc* mutants also increase phase shifts to light in the early evening. However, we found no difference in phase delays or advances between *Pdf* > *dnc* and control flies (data not shown), suggesting that altered light-responses of *dnc* hypomorphs are due to *dnc* acting in other clock neurons. The period-altering effects we see when manipulating cAMP levels are also consistent with data from Shafer et al. (2008) who found that expressing the cAMP-binding domain of mammalian Epac1 in LN_vs lengthens period. This Epac1 domain likely reduces free cAMP levels in LN_vs, although presumably not as potently as *UAS-dnc*. Third, mutations in PKA catalytic or regulatory subunits that affect the whole fly disrupt circadian behavior (Levine et al., 1994; Majercak et al., 1997; Park et al., 2000). Fourth, over-expressing a PKA catalytic subunit in LN_vs rescues the period-altering effect of a *UAS-shibire* transgene that alters vesicle recycling, although the PKA catalytic subunit had no effect by itself (Kilman et al., 2009). The long periods we observed with reduced Gs signaling in LN_vs also parallel mammalian studies in which pharmacologically reducing Adenylate cyclase activity lengthened period in SCN explants and mice (O'Neill et al., 2008).

G-proteins typically transduce extracellular signals. What signals could activate Gs in s-LN_vs? PDF is one possibility since PDFR induces cAMP signaling in response to PDF *in vitro*, indicating that it likely couples to Gs (Hyun et al., 2005; Lear et al., 2005). PDF could signal in an autocrine manner since PDFR is present in LN_vs (Im and Taghert, 2010). However, the long-periods we observed with reduced Gs signaling differ from the short-period and arrhythmic phenotypes of *Pdf* and *pdfR* mutants. The likeliest explanation for these differences is that the altered behavior of *Pdf* and *pdfR* mutants results from effects of PDF signaling over the entire circadian circuit (Peng et al., 2003; Shafer et al., 2008), whereas our manipulations specifically targeted LN_vs. Indeed, LN_vs are not responsible for the short-period rhythms in *Pdf*⁰¹ null mutant flies (Yoshii et al., 2009). Other possible explanations for the differences between the long-period rhythms with decreased Gs signaling in LN_vs and the short-period rhythms of *Pdf* and *pdfR* mutants are that additional GPCRs couple to Gs in s-LN_vs and influence molecular clock speed and that our manipulations decrease rather than abolish reception of PDF. In summary, our data shows that Gs signaling via cAMP in s-LN_vs modulates period length.

Go and GABAergic signaling help generate 24hr periods

Go signaling via PLC21C constitutes a novel pathway that regulates the s-LN_v molecular clock. We found that Go and the metabotropic GABA_B-R3 receptor are required for the

inhibitory effects of GABA on larval LN_vs, which develop into adult s-LN_vs (Kaneko et al., 1997). The same genetic manipulations that block GABA inhibition of LN_vs in culture (expression of *Ptx* or *GABA_B-R3-RNAi*) lengthened the period of adult locomotor rhythms. Furthermore, the molecular clock in s-LN_vs is disrupted when a subset of GABAergic neurons are hyper-excited. Since the LN_vs do not produce GABA themselves (Hamasaka et al., 2005 and Fig. 6B), s-LN_vs require GABAergic inputs to generate 24hr rhythms. Thus s-LN_vs are less autonomous for determining period length in DD than previously anticipated (Stoleru et al., 2005).

Activation of G-proteins can have both short- and long-term effects on a cell. With Go signaling blocked by Ptx, we detected short-term effects on LN_v responses to excitatory ACh and longer-term effects on the molecular clock. The latter are presumably explained by PLC activation since the behavioral phenotypes of *Pdf > GoGTP* flies were rescued by reducing *Plc21C* expression.

Since s-LN_v clocks were unchanged even when the speed of all non-LN_v clock neurons were genetically manipulated (Stoleru et al., 2005), it is surprising to find s-LN_v clocks altered by signaling from GABAergic non-clock neurons. Why would LN_vs need inputs from non-clock neurons to generate 24hr rhythms? One possibility is that LN_vs receive multiple inputs which either accelerate or slow down the pace of their molecular clock but overall balance each other to achieve 24hr rhythms in DD. Since reducing signaling by Gs and Go lengthens period, these pathways normally accelerate the molecular clock. According to this model, there are unidentified inputs to LN_vs which delay the clock. Identifying additional receptors in LN_vs would allow this idea to be tested.

Previous work showed that GABAergic neurons project to LN_vs (Hamasaka et al., 2005) and that GABA_A receptors in l-LN_vs regulate sleep (Chung et al., 2009; Parisky et al., 2008). Our data show that constitutive activation of Go signaling dramatically alters behavioral rhythms, suggesting that LN_vs normally receive rhythmic GABAergic inputs. But how can s-LN_vs integrate temporal information from non clock-containing GABAergic neurons? s-LN_vs could respond rhythmically to a constant GABAergic tone by controlling GABA_B-R3 activity. Indeed, a recent study found that *GABA_B-R3* RNA levels in s-LN_vs are much higher at ZT12 than at ZT0 (KulaEversole et al., 2010). Strikingly, this rhythm in *GABA_B-R3* expression is in antiphase to LN_v neuronal activity (Cao and Nitabach, 2008; Sheeba et al., 2008). Thus regulated perception of inhibitory GABAergic inputs could at least partly underlie rhythmic LN_v excitability. GABAergic inputs could also help synchronize LN_vs as in the cockroach circadian system (Schneider and Stengl, 2005). Thus GABA's short-term effects on LN_v excitability, likely mediated by Gβ/γ, and GABA's longer-term effects on the molecular clock via Go may both contribute to robust rhythms.

Conclusion

Our work adds to the growing network view of circadian rhythms in *Drosophila* where LN_vs integrate information to set period for the rest of the clock network in DD. The period-altering effects of decreased G-protein signaling in LN_vs point to a less hierarchical and more distributed network than previously envisioned. Since our data strongly suggests that GABA inputs are novel regulators of 24hr rhythms, the GABAergic neurons that fine-tune the s-LN_v clock should be considered part of the circadian network.

Experimental Procedures

Behavioral Analysis

Fly strains used are described in Supplementary Experimental procedures. For circadian locomotor behavior, flies were loaded into Trikinetics activity monitors and entrained to LD cycles for at least 3 days before transfer to DD. Data were analyzed by ClockLab in conjunction with MatLab. Period length was determined using the Lomb-Scargle algorithm and power determined by measuring the height of the peak at this period. Flies with a power >11 had significant rhythms ($p < .025$) while flies with power <11 were deemed arrhythmic. A two-tailed student t-test with equal variance was used to test differences in period length.

Immunostaining

Antibodies against PDF (1:50; DSHB), VRI (1:3000; from Paul Hardin), PER (1:5000; from Jeff Hall) and GFP (1:500; AbDSerotec) were used on adult brains as described (Collins et al., 2006). Three experiments were performed on different days with ≥ 8 brains and ≥ 16 clearly identifiable s-LN_vs analyzed per timepoint. Images were obtained on a Leica SP5 Confocal and Image J used to quantify pixel intensity. Since background staining of VRI and PER was <0.2 au for each condition, background was not subtracted from raw values (range: 2-75), which were pooled and averaged across experiments.

Live-cell Ca²⁺ imaging of dissociated *Drosophila* clock neurons

For each experiment, 30-60 3rd instar wandering larvae were collected at ZT9 and rinsed in dPBS. Larval brains were dissected, cleaned, rinsed and placed into dPBS on ice. After two brief rinses in dPBS and gentle centrifugation at 0.2 rcf, brains were re-suspended in 400 μ l of 1:1 mixture of dPBS: Schneider's S2 medium (Invitrogen) containing 2 Units/mL Dispase II (Roche). After 2hr at room temp, brains were washed twice in dPBS, re-suspended in 200 μ l S2 medium and dissociated by pipetting up and down 100x through a 200 μ l pipette tip. 50-65 μ l aliquots of the cell suspension were placed onto rectangular coverglass (Warner Instruments) and kept in a humidified dark chamber. Cells were allowed at least 2hr to attach to the coverglass before imaging and were discarded 12 hr after dissection.

The coverglass was mounted on an inverted Nikon TE2000U epifluorescence microscope via a small volume recording chamber (Warner Instruments). Neurons were illuminated at 480nm, 6nm bandpass using a monochromator (Photon Technology International) and fluorescent emission viewed through a 40x/0.60 Plan Fluor oil-immersion objective (Nikon) and standard FITC filter set (Chroma Technology). Cells were continuously superfused at 2 ml/min with standard saline (Jan and Jan, 1976) using a gravity-driven system. Chemicals were diluted in standard saline and a manual switching system used for solution exchange without interrupting flow to cells. Un-stimulated G-CaMP expressing neurons were located by their green emission and subsequent fluorescence summed over 2 second intervals was captured at 12-bit resolution via a CoolsnapFx CCD camera (Roper Scientific). Images were acquired and stored using Imaging Workbench 5.2 (INDEC Biosystems). Ovoid regions of interest were defined entirely within the fluorescent signal within each neuron tested and time-lapse numerical data obtained during *post-hoc* playback exported for further analysis in PRISM 4 (Graphpad). Physiology-grade salts and chemicals were from Fisher Scientific or Sigma Aldrich except for α -bungarotoxin from Tocris.

RNA analysis

Quantitative real time RT-PCR (qPCR) was used on RNA isolated at ZT9 from either whole heads or purified adult LN_vs. RNA was extracted using standard procedures for whole fly heads. To isolate RNA from adult LN_vs, brains were dissected starting at ZT9 from adult flies with *Pdf-RFP*, *Pdf-Gal4* and, for experimental flies, the *UAS-GABA β -R3:RNAi*

transgene. Brains were dissociated into a single-cell suspension as for Ca²⁺ imaging above and a 35µm nylon mesh filter (BD Falcon) used to remove cell clusters to minimize contamination by RFP⁻ cells attached to RFP⁺ cells. Cells in Schneider's medium / 10% FBS were kept on ice for transport to NYU School of Medicine FACS center for flow cytometry. We typically obtained ~300 RFP⁺ cells from ~50 adult brains, which were sorted directly into 500µl PicoPure Extraction Buffer and purified using the PicoPure RNA Isolation Kit (Molecular Devices). mRNA was amplified using the Nugen WT-Ovation™ Pico System to generate ~5µg single stranded amplified unlabeled cDNA product.

For qPCR reactions, 100ng of adult head RNA or 20ng LN_v cDNA was amplified in a Roche LightCycler using the Roche 2-step RT PCR RNA Master HybProbe Kit. RNA levels were determined by comparing when the reaction moved into detectable exponential phase with standard curves for each primer set constructed by re-amplifying known quantities of PCR products. We normalized the absolute level of each gene in an experiment to RNA levels of *Pdf* (a non-cycling transcript) in that experiment. Three biological replicates were averaged for RNA from whole heads and two for LN_v RNA. Primer and probe sequences are listed in Supplemental experimental procedures.

Supplementary Material

Refer to Web version on PubMed Central for supplementary material.

Acknowledgments

We thank Harold Atwood, Mike Forte, Leslie Griffith, Paul Hardin, Dierk Reiff, Andrew Tomlinson, Gregg Roman, Julie Simpson, Bloomington Stock Center, DSHB and the VDRC for flies and antibodies. We thank Chris Wegener, Gregg Roman and Mike Nitabach for advice suggestions. We also thank Karim Baroudy, Taniya Kaur and Alyson Knowles for help in initial stages of this project and Ben Collins for help with dissections. We thank Matthieu Cavey, Ben Collins, Alex Keene, Dogukan Mizrak, Afroditi Petsakou and Daniel Vasiliauskas for comments on the manuscript. Confocal images were obtained in the NYU Center for Genomics & Systems Biology. The investigation was largely conducted in a facility constructed with support from Research Facilities Improvement Grant Number C06 RR-15518-01 from NCR, NIH. The work was supported by NIH grants NS030808 (MA) and GM063911 (JB).

References

- Agosto J, Choi JC, Parisky KM, Stilwell G, Rosbash M, Griffith LC. Modulation of GABA_A receptor desensitization uncouples sleep onset and maintenance in *Drosophila*. *Nat Neurosci* 2008;11:354–359. [PubMed: 18223647]
- Albert JL, Lingle CJ. Activation of nicotinic acetylcholine receptors on cultured *Drosophila* and other insect neurones. *J Physiol* 1993;463:605–630. [PubMed: 7504110]
- Allada R, Emery P, Takahashi JS, Rosbash M. Stopping time: the genetics of fly and mouse circadian clocks. *Annu Rev Neurosci* 2001;24:1091–1119. [PubMed: 11520929]
- Balsalobre A, Damiola F, Schibler U. A serum shock induces circadian gene expression in mammalian tissue culture cells. *Cell* 1998;93:929–937. [PubMed: 9635423]
- Blanchard FJ, Collins B, Cyran SA, Hancock DH, Taylor MV, Blau J. The transcription factor Mef2 is required for normal circadian behavior in *Drosophila*. *J Neurosci* 2010;30:5855–5865. [PubMed: 20427646]
- Cao G, Nitabach MN. Circadian control of membrane excitability in *Drosophila melanogaster* lateral ventral clock neurons. *J Neurosci* 2008;28:6493–6501. [PubMed: 18562620]
- Cheung US, Shayan AJ, Boulianne GL, Atwood HL. *Drosophila* larval neuromuscular junction's responses to reduction of cAMP in the nervous system. *J Neurobiol* 1999;40:1–13. [PubMed: 10398067]

- Chung BY, Kilman VL, Keath JR, Pitman JL, Allada R. The GABA_A receptor RDL acts in peptidergic PDF neurons to promote sleep in *Drosophila*. *Curr Biol* 2009;19:386–390. [PubMed: 19230663]
- Collins B, Mazzoni EO, Stanewsky R, Blau J. *Drosophila* CRYPTOCHROME is a circadian transcriptional repressor. *Curr Biol* 2006;16:441–449. [PubMed: 16527739]
- Cyran SA, Buchsbaum AM, Reddy KL, Lin MC, Glossop NR, Hardin PE, Young MW, Storti RV, Blau J. *vriille*, *Pdp1*, and *dClock* form a second feedback loop in the *Drosophila* circadian clock. *Cell* 2003;112:329–341. [PubMed: 12581523]
- Day JP, Dow JA, Houslay MD, Davies SA. Cyclic nucleotide phosphodiesterases in *Drosophila melanogaster*. *Biochem J* 2005;388:333–342. [PubMed: 15673286]
- Dodd AN, Gardner MJ, Hotta CT, Hubbard KE, Dalchau N, Love J, Assie JM, Robertson FC, Jakobsen MK, Goncalves J, et al. The *Arabidopsis* circadian clock incorporates a cADPR-based feedback loop. *Science* 2007;318:1789–1792. [PubMed: 18084825]
- Fei H, Chow DM, Chen A, Romero-Calderon R, Ong WS, Ackerson LC, Maidment NT, Simpson JH, Frye MA, Krantz DE. Mutation of the *Drosophila* vesicular GABA transporter disrupts visual figure detection. *J Exp Biol* 2010;213:1717–1730. [PubMed: 20435823]
- Ferris J, Ge H, Liu L, Roman G. G(o) signaling is required for *Drosophila* associative learning. *Nat Neurosci* 2006;9:1036–1040. [PubMed: 16845387]
- Glossop NR, Houl JH, Zheng H, Ng FS, Dudek SM, Hardin PE. VRILLE feeds back to control circadian transcription of *Clock* in the *Drosophila* circadian oscillator. *Neuron* 2003;37:249–261. [PubMed: 12546820]
- Hamasaka Y, Rieger D, Parmentier ML, Grau Y, Helfrich-Forster C, Nassel DR. Glutamate and its metabotropic receptor in *Drosophila* clock neuron circuits. *J Comp Neurol* 2007;505:32–45. [PubMed: 17729267]
- Hamasaka Y, Wegener C, Nassel DR. GABA modulates *Drosophila* circadian clock neurons via GABA_B receptors and decreases in calcium. *J Neurobiol* 2005;65:225–240. [PubMed: 16118795]
- Harmar AJ, Arimura A, Gozes I, Journot L, Laburthe M, Pisegna JR, Rawlings SR, Robberecht P, Said SI, Sreedharan SP, et al. International Union of Pharmacology. XVIII. Nomenclature of receptors for Vasoactive Intestinal Peptide and Pituitary Adenylate Cyclase-Activating Polypeptide. *Pharmacol Rev* 1998;50:265–270. [PubMed: 9647867]
- Harmar AJ, Marston HM, Shen S, Spratt C, West KM, Sheward WJ, Morrison CF, Dorin JR, Piggins HD, Reubi JC, et al. The VPAC₂ receptor is essential for circadian function in the mouse suprachiasmatic nuclei. *Cell* 2002;109:497–508. [PubMed: 12086606]
- Harrisingh MC, Wu Y, Lnenicka GA, Nitabach MN. Intracellular Ca²⁺ regulates free-running circadian clock oscillation *in vivo*. *J Neurosci* 2007;27:12489–12499. [PubMed: 18003827]
- Herzog ED, Takahashi JS, Block GD. *Clock* controls circadian period in isolated suprachiasmatic nucleus neurons. *Nat Neurosci* 1998;1:708–713. [PubMed: 10196587]
- Hille, B. Ion channels of excitable membranes. 3rd edn. Sinauer Associates; Sunderland, Mass.: 2001.
- Hyun S, Lee Y, Hong ST, Bang S, Paik D, Kang J, Shin J, Lee J, Jeon K, Hwang S, et al. *Drosophila* GPCR Han is a receptor for the circadian clock neuropeptide PDF. *Neuron* 2005;48:267–278. [PubMed: 16242407]
- Im SH, Taghert PH. PDF receptor expression reveals direct interactions between circadian oscillators in *Drosophila*. *J Comp Neurol* 2010;518:1925–1945. [PubMed: 20394051]
- Jan LY, Jan YN. Properties of the larval neuromuscular junction in *Drosophila melanogaster*. *J Physiol* 1976;262:189–214. [PubMed: 11339]
- Kaneko M, Helfrich-Forster C, Hall JC. Spatial and temporal expression of the *period* and *timeless* genes in the developing nervous system of *Drosophila*: newly identified pacemaker candidates and novel features of clock gene product cycling. *J Neurosci* 1997;17:6745–6760. [PubMed: 9254686]
- Katanaev VL, Ponzelli R, Semeriva M, Tomlinson A. Trimeric G protein-dependent frizzled signaling in *Drosophila*. *Cell* 2005;120:111–122. [PubMed: 15652486]
- Kaupmann K, Malitschek B, Schuler V, Heid J, Froestl W, Beck P, Mosbacher J, Bischoff S, Kulik A, Shigemoto R, et al. GABA_B-receptor subtypes assemble into functional heteromeric complexes. *Nature* 1998;396:683–687. [PubMed: 9872317]

- Kavanaugh MP, Varnum MD, Osborne PB, Christie MJ, Busch AE, Adelman JP, North RA. Interaction between tetraethylammonium and amino acid residues in the pore of cloned voltage-dependent potassium channels. *J Biol Chem* 1991;266:7583–7587. [PubMed: 2019588]
- Kilman VL, Zhang L, Meissner RA, Burg E, Allada R. Perturbing dynamin reveals potent effects on the *Drosophila* circadian clock. *PLoS ONE* 2009;4:e5235. [PubMed: 19384421]
- Kula-Eversole E, Nagoshi E, Shang Y, Rodriguez J, Allada R, Rosbash M. Surprising gene expression patterns within and between PDF-containing circadian neurons in *Drosophila*. *Proc Natl Acad Sci U S A* 2010;107:13497–13502. [PubMed: 20624977]
- Lakin-Thomas PL, Brody S. Circadian rhythms in *Neurospora crassa*: interactions between clock mutations. *Genetics* 1985;109:49–66. [PubMed: 3155701]
- Lear BC, Merrill CE, Lin JM, Schroeder A, Zhang L, Allada R. A G protein-coupled receptor, *groom-of-PDF*, is required for PDF neuron action in circadian behavior. *Neuron* 2005;48:221–227. [PubMed: 16242403]
- Levine JD, Casey CI, Kalderon DD, Jackson FR. Altered circadian pacemaker functions and cyclic AMP rhythms in the *Drosophila* learning mutant *dunce*. *Neuron* 1994;13:967–974. [PubMed: 7946340]
- Lin Y, Stormo GD, Taghert PH. The neuropeptide Pigment-Dispersing Factor coordinates pacemaker interactions in the *Drosophila* circadian system. *J Neurosci* 2004;24:7951–7957. [PubMed: 15356209]
- Liu AC, Welsh DK, Ko CH, Tran HG, Zhang EE, Priest AA, Buhr ED, Singer O, Meeker K, Verma IM, et al. Intercellular coupling confers robustness against mutations in the SCN circadian clock network. *Cell* 2007;129:605–616. [PubMed: 17482552]
- Liu C, Weaver DR, Strogatz SH, Reppert SM. Cellular construction of a circadian clock: period determination in the suprachiasmatic nuclei. *Cell* 1997;91:855–860. [PubMed: 9413994]
- Majercak J, Kalderon D, Edery I. *Drosophila melanogaster* deficient in Protein Kinase A manifests behavior-specific arrhythmia but normal clock function. *Mol Cell Biol* 1997;17:5915–5922. [PubMed: 9315649]
- Maywood ES, Reddy AB, Wong GK, O'Neill JS, O'Brien JA, McMahon DG, Harmor AJ, Okamura H, Hastings MH. Synchronization and maintenance of timekeeping in suprachiasmatic circadian clock cells by neuroptidergic signaling. *Curr Biol* 2006;16:599–605. [PubMed: 16546085]
- McCormack TJ. Comparison of K⁺-channel genes within the genomes of *Anopheles gambiae* and *Drosophila melanogaster*. *Genome Biol* 2003;4:R58. [PubMed: 12952537]
- Mehren JE, Griffith LC. Cholinergic neurons mediate CaMKII-dependent enhancement of courtship suppression. *Learn Mem* 2006;13:686–689. [PubMed: 17101876]
- Mertens I, Vandingenen A, Johnson EC, Shafer OT, Li W, Trigg JS, De Loof A, Schoofs L, Taghert PH. PDF receptor signaling in *Drosophila* contributes to both circadian and geotactic behaviors. *Neuron* 2005;48:213–219. [PubMed: 16242402]
- Mezler M, Muller T, Raming K. Cloning and functional expression of GABA_B receptors from *Drosophila*. *Eur J Neurosci* 2001;13:477–486. [PubMed: 11168554]
- Nagoshi E, Sugino K, Kula E, Okazaki E, Tachibana T, Nelson S, Rosbash M. Dissecting differential gene expression within the circadian neuronal circuit of *Drosophila*. *Nat Neurosci* 2010;13:60–8. [PubMed: 19966839]
- Nitabach MN, Blau J, Holmes TC. Electrical silencing of *Drosophila* pacemaker neurons stops the free-running circadian clock. *Cell* 2002;109:485–495. [PubMed: 12086605]
- Nitabach MN, Wu Y, Sheeba V, Lemon WC, Strumbos J, Zelensky PK, White BH, Holmes TC. Electrical hyperexcitation of lateral ventral pacemaker neurons desynchronizes downstream circadian oscillators in the fly circadian circuit and induces multiple behavioral periods. *J Neurosci* 2006;26:479–489. [PubMed: 16407545]
- O'Neill JS, Maywood ES, Chesham JE, Takahashi JS, Hastings MH. cAMP-dependent signaling as a core component of the mammalian circadian pacemaker. *Science* 2008;320:949–953. [PubMed: 18487196]
- Olsen SR, Wilson RI. Lateral presynaptic inhibition mediates gain control in an olfactory circuit. *Nature* 2008;452:956–960. [PubMed: 18344978]

- Parisky KM, Agosto J, Pulver SR, Shang Y, Kuklin E, Hodge JJ, Kang K, Liu X, Garrity PA, Rosbash M, Griffith LC. PDF cells are a GABA-responsive wake-promoting component of the *Drosophila* sleep circuit. *Neuron* 2008;60:672–682. [PubMed: 19038223]
- Park SK, Sedore SA, Cronmiller C, Hirsh J. Type II cAMP-dependent protein kinase-deficient *Drosophila* are viable but show developmental, circadian, and drug response phenotypes. *J Biol Chem* 2000;275:20588–20596. [PubMed: 10781603]
- Peng Y, Stoleru D, Levine JD, Hall JC, Rosbash M. *Drosophila* free-running rhythms require intercellular communication. *PLoS Biol* 2003;1:E13. [PubMed: 12975658]
- Pollack I, Hofbauer A. Histamine-like immunoreactivity in the visual system and brain of *Drosophila melanogaster*. *Cell Tissue Res* 1991;266:391–398. [PubMed: 1684918]
- Reiff DF, Ihring A, Guerrero G, Isacoff EY, Joesch M, Nakai J, Borst A. *In vivo* performance of genetically encoded indicators of neural activity in flies. *J Neurosci* 2005;25:4766–4778. [PubMed: 15888652]
- Renn SC, Park JH, Rosbash M, Hall JC, Taghert PH. A *pdf* neuropeptide gene mutation and ablation of PDF neurons each cause severe abnormalities of behavioral circadian rhythms in *Drosophila*. *Cell* 1999;99:791–802. [PubMed: 10619432]
- Reppert SM, Weaver DR. Coordination of circadian timing in mammals. *Nature* 2002;418:935–941. [PubMed: 12198538]
- Rothenfluh A, Abodeely M, Young MW. Short-period mutations of *per* affect a double-time-dependent step in the *Drosophila* circadian clock. *Curr Biol* 2000;10:1399–1402. [PubMed: 11084344]
- Schneider NL, Stengl M. Pigment-dispersing factor and GABA synchronize cells of the isolated circadian clock of the cockroach *Leucophaea maderae*. *J Neurosci* 2005;25:5138–5147. [PubMed: 15917454]
- Shafer OT, Kim DJ, Dunbar-Yaffe R, Nikolaev VO, Lohse MJ, Taghert PH. Widespread receptivity to neuropeptide PDF throughout the neuronal circadian clock network of *Drosophila* revealed by real-time cyclic AMP imaging. *Neuron* 2008;58:223–237. [PubMed: 18439407]
- Sheeba V, Fogle KJ, Kaneko M, Rashid S, Chou YT, Sharma VK, Holmes TC. Large ventral lateral neurons modulate arousal and sleep in *Drosophila*. *Curr Biol* 2008;18:1537–1545. [PubMed: 18771923]
- Shortridge RD, Yoon J, Lending CR, Bloomquist BT, Perdew MH, Pak WL. A *Drosophila* phospholipase C gene that is expressed in the central nervous system. *J Biol Chem* 1991;266:12474–12480. [PubMed: 2061323]
- Stanewsky R, Jamison CF, Plautz JD, Kay SA, Hall JC. Multiple circadian-regulated elements contribute to cycling *period* gene expression in *Drosophila*. *EMBO J* 1997;16:5006–5018. [PubMed: 9305642]
- Stoleru D, Peng Y, Nawathean P, Rosbash M. A resetting signal between *Drosophila* pacemakers synchronizes morning and evening activity. *Nature* 2005;438:238–242. [PubMed: 16281038]
- Ueno K, Kohatsu S, Clay C, Forte M, Isono K, Kidokoro Y. *Gsα* is involved in sugar perception in *Drosophila melanogaster*. *J Neurosci* 2006;26:6143–6152. [PubMed: 16763022]
- Wegener C, Hamasaka Y, Nassel DR. Acetylcholine increases intracellular Ca^{2+} via nicotinic receptors in cultured PDF-containing clock neurons of *Drosophila*. *J Neurophysiol* 2004;91:912–923. [PubMed: 14534288]
- Welsh DK, Logothetis DE, Meister M, Reppert SM. Individual neurons dissociated from rat suprachiasmatic nucleus express independently phased circadian firing rhythms. *Neuron* 1995;14:697–706. [PubMed: 7718233]
- Wolfgang WJ, Roberts IJ, Quan F, O'Kane C, Forte M. Activation of protein kinase A-independent pathways by $G_s\alpha$ in *Drosophila*. *Proc Natl Acad Sci U S A* 1996;93:14542–14547. [PubMed: 8962088]
- Yasuyama K, Meinertzhagen IA. Extraretinal photoreceptors at the compound eye's posterior margin in *Drosophila melanogaster*. *J Comp Neurol* 1999;412:193–202. [PubMed: 10441750]
- Yoshii T, Wulbeck C, Sehadova H, Veleri S, Bichler D, Stanewsky R, HelfrichForster C. The neuropeptide Pigment-Dispersing Factor adjusts period and phase of *Drosophila's* clock. *J Neurosci* 2009;29:2597–2610. [PubMed: 19244536]

Yuan Q, Lin F, Zheng X, Sehgal A. Serotonin modulates circadian entrainment in *Drosophila*. *Neuron* 2005;47:115–127. [PubMed: 15996552]

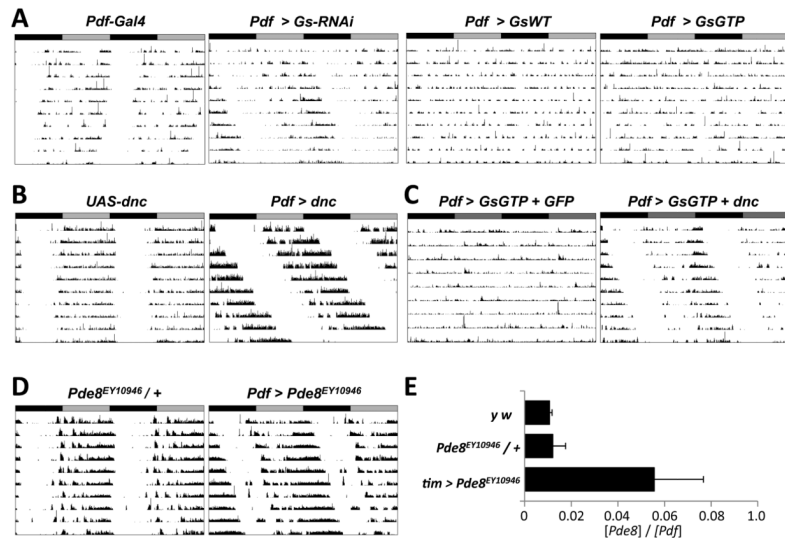


Figure 1. Normal Gs signaling in LN_vs is required for 24hr locomotor rhythms

A-D: Representative actograms showing locomotor activity in DD of flies with manipulations to Gs signaling in LN_vs. Actograms are double-plotted with gray and black bars indicating prior LD cycles.

(A) Left: Control fly homozygous for two *Pdf-Gal4* transgenes with 24.0hr period. The next three panels (from left to right) show activity of flies with *Pdf-Gal4* expressing transgenes with RNAi directed against *Gs* (*Pdf > Gs-RNAi*), wild type *Gs* (*Pdf > Gs*) or constitutively active *Gs* (*Pdf > Gs-GTP*). *Pdf > Gs-RNAi* flies had longer period rhythms (25.0hr) than controls ($p < .0001$ vs *PdfGal4* and *UAS-Gs-RNAi / +* flies). *Pdf > Gs* and *Pdf > Gs-GTP* flies were either arrhythmic or had weaker rhythms than controls.

(B) Left: fly with a *UAS-dnc* transgene (*UAS-dnc*, 24.0hr). Right: fly with *UAS-dnc* expressed in LN_vs (*Pdf > dnc*, 26.6hr). *Pdf > dnc* flies have longer periods than controls ($p < .001$).

(C) Flies with *Pdf-Gal4* expressing *UAS-Gs-GTP* and either a *UAS-CD8::GFP* transgene (*Pdf > GsGTP + GFP*, left) or a *UAS-dnc* transgene (*Pdf > GsGTP + dnc*, right).

(D) Left: Fly heterozygous for a P-element in *Pde8* (*Pde8^{EY10946} / +*, 24.2hr). Right: Fly with *Pde8* mis-expressed in LN_vs (*Pdf > Pde8^{EY10946}*, 25.0hr, right). *Pdf > Pde8^{EY10946}* flies have longer periods than controls ($p < .001$).

(E) RNA was isolated from heads of *y w* and *Pde8^{EY10946} / +* control flies and from flies with *tim(UAS)-Gal4* mis-expressing *Pde8^{EY10946}* (*tim > Pde8^{EY10946}*). Levels of *Pde8* and *Pdf* RNA were measured by qPCR and the relative level ($Pde8 : Pdf$) plotted, with error bars showing SEM. Since *tim > Pde8^{EY10946}* flies have more *Pde8* RNA than controls ($p < 0.01$), Gal4-activated *Pde8^{EY10946}* mis-expresses *Pde8*.

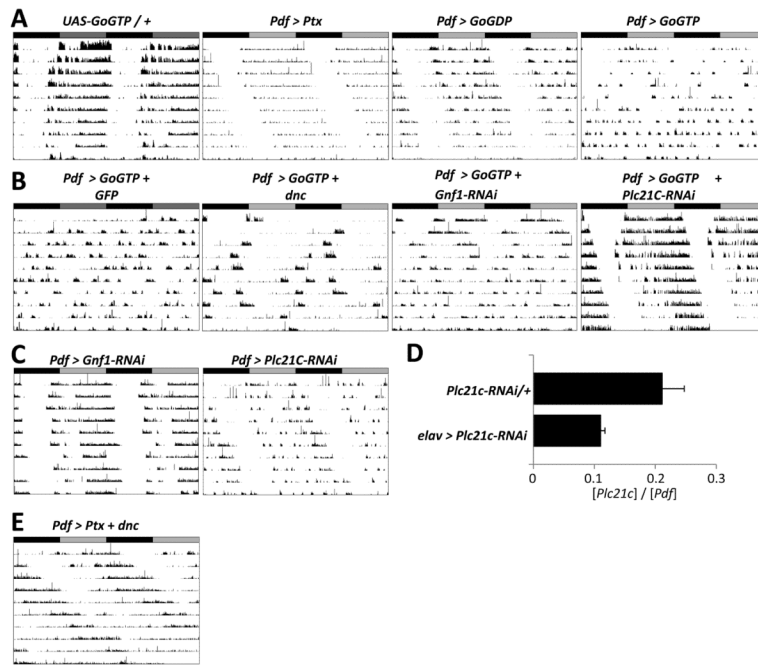


Figure 2. Go signaling in LN_vs requires *Plc21C* for 24hr behavioral rhythms

Representative actograms for flies in DD as in Figure 1.

(A) Left: A control fly heterozygous for a constitutively active *Go* transgene (*UAS-Go-GTP* / +, 23.6 hr). The next panels (left to right) show activity of flies with *Pdf-Gal4* expressing transgenes with Pertussis toxin (*Pdf > Ptx*, 25.2hr), constitutively inactive *Go* (*Pdf > Go-GDP*, 25.0hr) or constitutively active *Go* (*Pdf > Go-GTP*). *Pdf > Ptx* and *Pdf > Go-GDP* flies had significantly longer rhythms than controls ($p < .001$ vs *Pdf-Gal4*). *Pdf > Go-GTP* flies either became arrhythmic during DD or had shorter rhythms than control flies (22.3hr, $p < .001$ vs *Pdf-Gal4* and *UAS-Go-GTP* / + flies).

(B) *Pdf > Go-GTP* flies expressing a third transgene. From left to right: *UAS-CD8::GFP* control (*Pdf > Go-GTP + GFP*), *UAS-dnc* (*Pdf > Go-GTP + dnc*), control RNAi to *Gnf1* (*Pdf > Go-GTP + Gnf1-RNAi*) and RNAi to *Plc21C* (*Pdf > Go-GTP + Plc21C-RNAi*). *Pdf > Go-GTP + Plc21C-RNAi* flies had stronger rhythms than *Pdf > Go-GTP + Gnf1-RNAi* flies ($p < .001$).

(C) Flies with a control RNAi (*Pdf > Gnf1-RNAi*, 24.3hr, left) or RNAi against *Plc21C* (*Pdf > Plc21C-RNAi*, 25.1hr, right). *Pdf > Plc21C-RNAi* flies have longer periods than control flies ($p < .001$ vs *Pdf > Gnf1*).

(D) qPCR on RNA isolated from adult fly heads from either *UAS-Plc21C-RNAi* / + heterozygotes or flies with *elav-Gal4* expressing *UAS-Plc21C-RNAi* in post-mitotic neurons (*elav > Plc21C-RNAi*). The relative levels of *Plc21C* and *Pdf* RNA are plotted. *elav > Plc21C-RNAi* flies have less *Plc21C* RNA than controls ($p = 0.05$).

(E) Locomotor activity of a fly co-expressing *UAS-dnc* and *UAS-Ptx* in LN_vs (*Pdf > dnc + Ptx*). *Pdf > dnc + Ptx* flies had longer periods (28.4hr) than *Pdf > dnc* and *Pdf > Ptx* flies ($p < .001$).

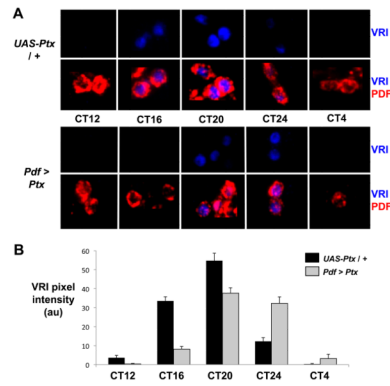


Figure 3. Molecular clock progression is delayed by inhibiting Go signaling

(A) Representative confocal images of s-LN_{v,s} on days 3–4 in DD stained for VRI (blue) and PDF (red) in *UAS-Ptx* / + control flies (top panels) and *Pdf* > *Ptx* flies (bottom). Data is quantified in (B) for *UAS-Ptx* / + controls (black) and *Pdf* > *Ptx* (gray) with error bars showing SEM.

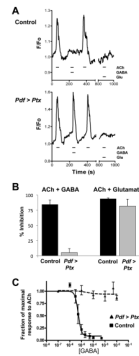


Figure 4. Go is required for the inhibitory effects of GABA on larval LN_vs

(A) Representative fluorescence measurements from dissociated larval LN_vs when 10μM acetylcholine (ACh) was applied alone or together with 100μM GABA or glutamate (Glu). Upper traces are LN_vs with *Pdf-Gal4* expressing *UAS-G-CaMP* (Control). Lower traces are LN_vs with *Pdf-Gal4* expressing *UAS-G-CaMP* and *UAS-Ptx* (*Pdf* > *Ptx*).

(B) Quantitation of inhibition by GABA (left) or glutamate (right) of 10μM ACh-induced Ca²⁺-responses for Control (black) and *Pdf* > *Ptx* (gray) LN_vs. Ptx prevented GABA-mediated inhibition ($p < .001$ vs *Pdf* > *G-CaMP*, $n = 9$) but had no effect on glutamate inhibition ($p > .2$, $n = 5$). (C) Dose-response curve for GABA on Control (squares, solid line) and *Pdf* > *Ptx* (triangles, dashed line) LN_vs. IC₅₀ for control LN_vs is 3.8μM but was unmeasurable for *Pdf* > *Ptx* LN_vs.

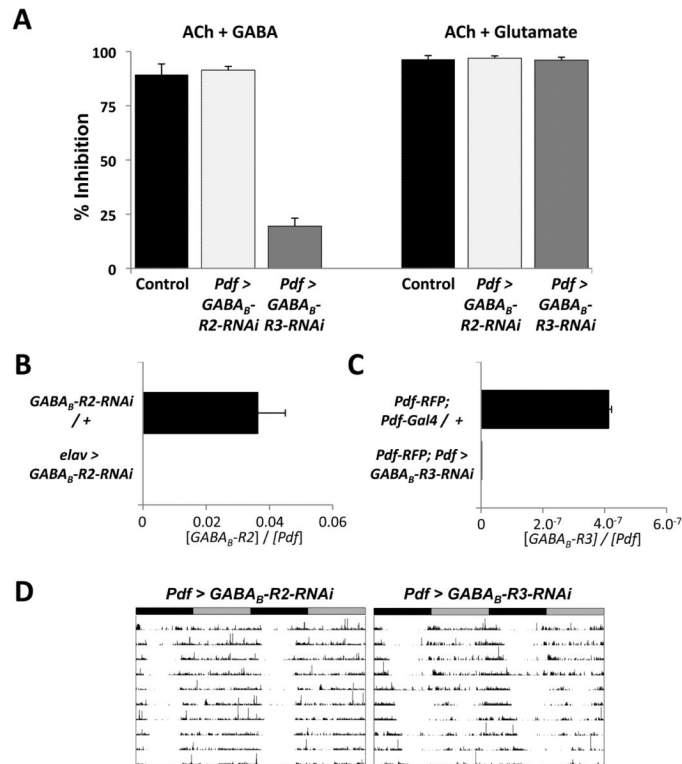


Figure 5. RNAi to the metabotropic GABA receptor GABA_B-3 subunit reduces inhibition by GABA and lengthens period of adult locomotor rhythms

(A) Quantification of inhibition of Ca²⁺-responses for ACh + GABA (left) or ACh + glutamate (right) compared to ACh. LN_vs from larvae with *Pdf-Gal4* and *UAS-G-CaMP* and either no other transgenes (Control, black bars, 89% inhibition), *UAS-GABA_B-R2-RNAi* on Chr. III (*Pdf > GABA_B-R2-RNAi*, light gray, 91% inhibition, *p* > .5 vs Control) or *UAS-GABA_B-R3-RNAi* (*Pdf > GABA_B-R3-RNAi*, dark gray, 19.5% inhibition, *p* < .001 vs Control). (B) Adult head RNA levels of *GABA_B-R2* and *Pdf* were measured as in Figure 2 from either *UAS-GABA_B-R2-RNAi* heterozygotes (*GABA_B-R2-RNAi / +*) or flies with *elav-Gal4* expressing *UAS-GABA_B-R2-RNAi* (*elav > GABA_B-R2-RNAi*). *GABA_B-R2* RNA levels were lower in *elav > GABA_B-R2-RNAi* flies (*p* < 0.01). (C) *GABA_B-R3* and *Pdf* RNA levels measured by qPCR on amplified RNA from adult LN_vs isolated from *Pdf-RFP; Pdf-Gal4 / +* controls or flies which also had *UAS-GABA_B-R3-RNAi* (*Pdf-RFP; Pdf > GABA_B-R3-RNAi*). *GABA_B-R3* RNA levels were reduced in *Pdf-RFP; Pdf > GABA_B-R3-RNAi* flies (*p* < 0.02). *Pdf* RNA levels were ~2.5-fold higher with *GABA_B-R3-RNAi* flies and so the extent of knockdown with this RNAi transgene (>400-fold) may be over-estimated. (D) Representative actograms of adult flies expressing either *GABA_B-R2-RNAi* (*Pdf > GABA_B-R2-RNAi*, left) or *GABA_B-R3-RNAi* (*Pdf > GABA_B-R3-RNAi*, right) in LN_vs. *Pdf > GABA_B-R3-RNAi* flies have longer period rhythms than *Pdf > GABA_B-R2-RNAi* flies (24.9hr vs 24.3hr, *p* < .001).

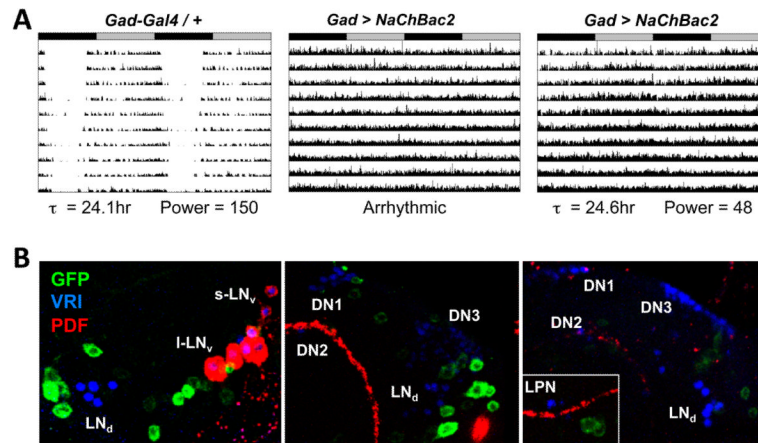


Figure 6. Hyper-exciting GABAergic neurons causes behavioral arrhythmicity

(A) Representative actograms of heterozygous control *Gad-Gal4 / +* fly (left) and two flies with *Gad-Gal4* expressing *UAS-NaChBac2* (*Gad > NaChBac2*, center and right). ClockLab marked the *Gad > NaChBac2* center fly as arrhythmic while the fly on the right as having a period of 24.6hr and a low power rhythm. Rhythmic *Gad > NaChBac2* flies had weaker power rhythms than control flies ($p < .001$).

(B) Localization of *Gad-Gal4* expression using a *UAS-CD8::GFP* reporter in three individual brains stained at ZT20 with antibodies to GFP (green), VRI (blue, marks all clock neurons) and PDF (red). Although some GFP+ neurons are close to VRI+ clock neurons, there is no obvious co-localization of VRI and GFP. Images are representative of 13 brain lobes.

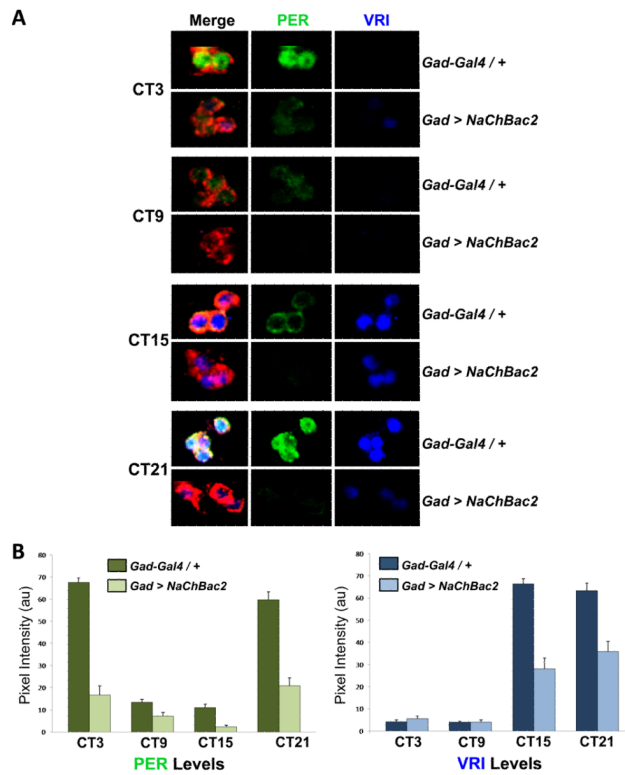


Figure 7. Hyper-exciting GABAergic neurons disrupts s-LN_v molecular rhythms
 (A) Representative confocal images of s-LN_vs at 4 timepoints on day 3 in DD using antibodies to PER (green), VRI (blue), and PDF (red) in *Gad-Gal4 / +* control flies (top panels) and *Gad > NaChBac2* flies (bottom panels). Data are quantified in (B) for *Gad-Gal4 / +* controls (dark green and dark blue bars for PER and VRI respectively) and for *Gad > NaChBac2* (light green and light blue) with SEM shown. Experiments were carried out on 3 separate days with at least 12 brains and 30 clearly identifiable s-LN_vs measured in total.

Table 1
Locomotor rhythms in DD for flies with altered Gs and Go signaling in LN_vs

The nomenclature *Pdf*> *X* indicates that two copies of *Pdf*_{0.5}-*Gal4* (Park et al., 2000) were used to express *UAS-X*. *Pdf*> *X* + *Y* indicates simultaneous expression of *UAS-X* and *UAS-Y*. n: number of flies assayed. % ar: percentage of arrhythmic flies. Period is shown in hr for rhythmic flies with standard error of the mean (SEM). Power indicates rhythm strength with its SEM.

Genotype	n	% ar	Period (hr) ± SEM	Power ± SEM
<i>Pdf-Gal4</i>	15	0	24.0 ± 0.1	102 ± 23.8
<i>Pdf</i> > <i>Gs-RNAi</i>	31	0	25.0 ± 0.1	113.8 ± 13.0
<i>Pdf</i> > <i>Gs</i>	20	65	24.2 ± 0.2	36.8 ± 9.3
<i>Pdf</i> > <i>Gs-GTP</i>	26	62	24.0 ± 0.1	14.5 ± 2.6
<i>Pdf</i> > <i>dnc</i>	38	0	26.6 ± 0.1	317.1 ± 26.5
<i>Pdf</i> > <i>Pde8^{EY10946}</i>	16	6	25.0 ± 0.1	200.3 ± 22.1
<i>UAS-Gs-RNAi</i> / +	27	4	23.8 ± 0.1	75.4 ± 6.8
<i>UAS-Gs</i> / +	19	5	24.5 ± 0.1	76.2 ± 10.9
<i>UAS-Gs-GTP</i> / +	16	6	24.1 ± 0.1	77.3 ± 16.0
<i>UAS-dnc</i> / +	28	0	24.0 ± 0.1	221.8 ± 18.5
<i>Pde8^{EY10946}</i> / +	15	0	24.2 ± 0.1	170.8 ± 17.9
<i>Pdf</i> > <i>Gs-GTP</i> + <i>dnc</i>	20	0	24.7 ± 0.1	197.1 ± 24.7
<i>Pdf</i> > <i>Gs-GTP</i> + <i>CD8::GFP</i>	19	21	23.4 ± 0.3	74.1 ± 10.3
<i>Pdf</i> > <i>Ptx</i>	36	0	25.2 ± 0.1	67.8 ± 6.6
<i>Pdf</i> > <i>Go-GDP</i>	49	4	25.0 ± 0.1	100.8 ± 10.1
<i>Pdf</i> > <i>Go-GTP</i>	26	46	22.3 ± 0.3	24.8 ± 2.3
<i>UAS-Ptx</i> / +	17	12	23.8 ± 0.1	66.9 ± 12.7
<i>UAS-Go-GTP</i> / +	16	0	23.6 ± 0.1	130.1 ± 16.7
<i>UAS-Go-GDP</i> / +	12	0	23.8 ± 0.1	136.5 ± 33.1
<i>Pdf</i> > <i>Go-GTP</i> + <i>CD8::GFP</i>	11	55	22.6 ± 0.2	39.7 ± 10.1
<i>Pdf</i> > <i>Go-GTP</i> + <i>Plc21C-RNAi</i>	22	0	24.7 ± 0.1	199.7 ± 17.9
<i>Pdf</i> > <i>Go-GTP</i> + <i>Gnf1-RNAi</i>	12	17	22.8 ± 0.3	61.4 ± 11.4
<i>Pdf</i> > <i>Go-GTP</i> + <i>dnc</i>	13	23	21.6 ± 0.1	48.5 ± 7.3
<i>Pdf</i> > <i>dnc</i> + <i>Ptx</i>	26	8	28.4 ± 0.1	104.4 ± 14.3
<i>Pdf</i> > <i>Plc21C-RNAi</i>	29	0	25.1 ± 0.1	195.6 ± 17.3
<i>Pdf</i> > <i>Gnf1-RNAi</i>	14	7	24.3 ± 0.1	118.2 ± 10.4
<i>Pdf</i> > <i>GABA_B-R2-RNAi</i> (1784)	30	0	24.3 ± 0.1	160.5 ± 10.9
<i>Pdf</i> > <i>GABA_B-R2-RNAi</i> (1785)	22	0	24.2 ± 0.1	78.6 ± 8.4
<i>Pdf</i> > <i>GABA_B-R3-RNAi</i>	21	0	24.9 ± 0.1	92.5 ± 14.6
<i>UAS-GABA_B-R3-RNAi</i> / +	14	0	23.8 ± 0.1	56.7 ± 11.7
<i>UAS-NaChBac2</i> / +	16	6	24.1 ± 0.1	112.5 ± 18.4
<i>Gad-Gal4</i> / +	15	7	24.0 ± 0.2	119.4 ± 19.9
<i>Gad</i> > <i>NaChBac2</i>	31	39	24.3 ± 0.3	38.6 ± 5.2